Neuropsychologia 141 (2020) 107433

Contents lists available at ScienceDirect

Neuropsychologia

journal homepage: http://www.elsevier.com/locate/neuropsychologia

Dissociable effects of tDCS polarity on latent decision processes are associated with individual differences in neurochemical concentrations and cortical morphology

Hannah L. Filmer [a,*], Timothy Ballard [a], Shane E. Ehrhardt [a], Saskia Bollmann [b], Thomas B. Shaw [b], Jason B. Mattingley [a,c,d], Paul E. Dux [a]

[a] School of Psychology, The University of Queensland, St Lucia, Australia
[b] Centre for Advanced Imaging, The University of Queensland, St Lucia, Australia
[c] Queensland Brain Institute, The University of Queensland, St Lucia, Australia
[d] Canadian Institute for Advanced Research (CIFAR), Toronto, Canada

ARTICLE INFO

Keywords:
tDCS
Individual differences
Computational modelling
Neurochemicals
Cortical structure

ABSTRACT

Applying a weak electrical current to the cortex has the potential to modulate neural functioning and behaviour. The most common stimulation technique, transcranial direct current stimulation (tDCS), has been used for causal investigations of brain and cognitive functioning, and to treat psychiatric conditions such as depression. However, the efficacy of tDCS in modulating behaviour varies across individuals. Moreover, despite being associated with different neural effects, the two polarities of electrical stimulation – anodal and cathodal – can result in similar behavioural outcomes. Here we employed a previously replicated behavioural paradigm that has been associated with polarity non-specific disruption of training effects in a simple decision-making task. We then used the linear ballistic accumulator model to quantify latent components of the decision-making task. In addition, magnetic resonance imaging measures were acquired prior to tDCS sessions to quantify cortical morphology and local neurochemical concentrations. Both anodal and cathodal stimulation disrupted learning-related task improvement relative to sham (placebo) stimulation, but the two polarities of stimulation had distinct effects on latent task components. Whereas anodal stimulation tended to affect decision thresholds for the behavioural task, cathodal stimulation altered evidence accumulation rates. Moreover, performance variability with anodal stimulation was related to cortical thickness of the inferior frontal gyrus, whereas performance variability with cathodal stimulation was related to cortical thickness in the inferior precentral sulcus, as well as to prefrontal neurochemical excitability. Our findings demonstrate that both cortical morphology and local neurochemical balance are important determinants of individual differences in behavioural responses to electrical brain stimulation.

1. Introduction

Transcranial direct current stimulation (tDCS) involves running a small electrical current between two or more electrodes placed on the scalp. The current is directional, flowing between positive (anodal) and negative (cathodal) terminals. The technique is particularly useful for determining the causal role of local cortical regions and their associated perceptual, cognitive or motor functions (for a review, see Filmer et al., 2014). In the context of the present study, tDCS of the prefrontal cortex – implicated in a range of executive processes (Roberts et al., 1998) – has shown promise for the treatment of depression (Brunoni et al., 2017; Nord et al., 2019), attenuating cognitive decline in older adults (Stephens and Berryhill, 2016), and enhancing the benefits of cognitive training in healthy young adults (Filmer et al., 2017a, 2017b; Filmer et al., 2017a, 2017b).

Distinct cortical effects have been associated with each stimulation polarity. Specifically, cortex proximal to the anodal electrode shows increased excitability (Nitsche and Paulus, 2000a) and decreased concentrations of the inhibitory neurochemical gamma-aminobutyric acid (GABA; Bachtiar et al., 2018; Bachtiar et al., 2015; Stagg et al., 2009;

* Corresponding author. McElwain Building, Campbell Road, St Lucia, 4072, Australia.
E-mail address: h.l.filmer@gmail.com (H.L. Filmer).

https://doi.org/10.1016/j.neuropsychologia.2020.107433
Received 16 September 2019; Received in revised form 2 March 2020; Accepted 9 March 2020
Available online 14 March 2020
0028-3932/

Stagg et al., 2011). In contrast, cortex proximal to the cathodal electrode shows decreased excitability (Nitsche and Paulus, 2000a; though this varies with stimulation intensity/duration, Samani, et al., 2019) and reduced concentrations of the excitatory neurochemical glutamate (Stagg et al., 2009). The issue of stimulation polarity is likely to be more nuanced, and dependent on factors such as the orientations of the affected neurons (Liu et al., 2018). Moreover, the effects of tDCS are variable across subjects (Wiethoff et al., 2014), potentially limiting applications (Parkin et al., 2015). However, such individual variability can be harnessed to help relate brain function (Drew and Vogel, 2008; Garner and Dux, 2015), structure (Frank et al., 2016; Kanai et al., 2010; Verghese et al., 2016), and neurochemical concentration (Terhune et al., 2014; Yoon et al., 2016) to behaviour. In addition, baseline neural activity can predict patient response to tDCS treatment for depression (Nord et al., 2019). If the sources of variability in tDCS outcomes are characterised, interventions may be tailored to maximise benefits.

We have previously shown that both anodal and cathodal stimulation with tDCS can disrupt learning in a decision-making task when applied offline over the left prefrontal cortex (Filmer et al., 2013a, 2013b; Filmer et al., 2013a, 2013b), suggesting that tDCS may have similar behavioural effects regardless of stimulation polarity (see also Stagg et al., 2011). It remains unclear, however, whether the two polarities might differentially modulate latent components of the decision-making process which cannot be accessed using response time and accuracy measures alone. Computational models of choice and response time, such as the linear ballistic accumulator framework (LBA; Brown and Heathcote, 2008), can quantify these latent components – specifically, the *drift rate* (the rate at which evidence is accumulated for response options), the *response threshold* (the amount of evidence required for a decision to be reached), and non-decision time (a combination of sensory and motor processes). By quantifying latent components, it is possible to obtain a more mechanistic characterisation of how stimulation modulates behavioural outcomes.

Here, we employed our previously replicated decision-making paradigm (Filmer et al., 2013a, 2013b) to ascertain the effect of stimulation on latent decision processes. The effects of stimulation were modelled for each subject, and related to baseline measures of local neurochemical concentrations (using magnetic resonance spectroscopy; MRS) and cortical morphology (using magnetic resonance imaging; MRI). We expected both anodal and cathodal tDCS to disrupt training related gains in reaction times, and for this to be reflected in modulations of latent decision processes (thresholds and/or drift rates). Using an individual differences approach, stimulation effects on decision processes were expected to relate to both cortical thickness and neurochemical concentrations in the left prefrontal cortex. The specific nature of these relationships were not predicted in advance, and hence this element of the study was exploratory. To preview the results, we replicated our finding of polarity non-specific disruption of training benefits on the decision-making task, but also revealed distinct effects of stimulation polarity on latent decision components: whereas anodal stimulation predominantly affected subjects' response thresholds, cathodal stimulation affected the rate of evidence accumulation. Moreover, we found that variability in the effect of tDCS on decision-making was associated with individual differences in both cortical thickness and local neurochemical concentrations in the prefrontal cortex.

2. Method

2.1. Overview

The data were collected for a large-scale project aimed at investigating factors relating to tDCS efficacy, some elements of which have been reported previously (Filmer et al., 2019a, 2019b; Filmer et al., 2019a, 2019b). Here, we used LBA modelling to identify the different latent processes that contribute to decision-making and assess group level effects of tDCS on these, as well as how individual differences in latent process responses to stimulation relate to prefrontal neurochemical metabolites and cortical structure. Subjects each completed four separate experimental sessions on different days (see Fig. 1). The first session measured cortical structure and baseline concentrations of neurochemicals using MRI and MRS, respectively. The second, third, and fourth sessions implemented a replication of a previous paradigm (Filmer et al., 2013a, 2013b), in which decision-making training was undertaken under conditions of anodal, cathodal, and sham tDCS.

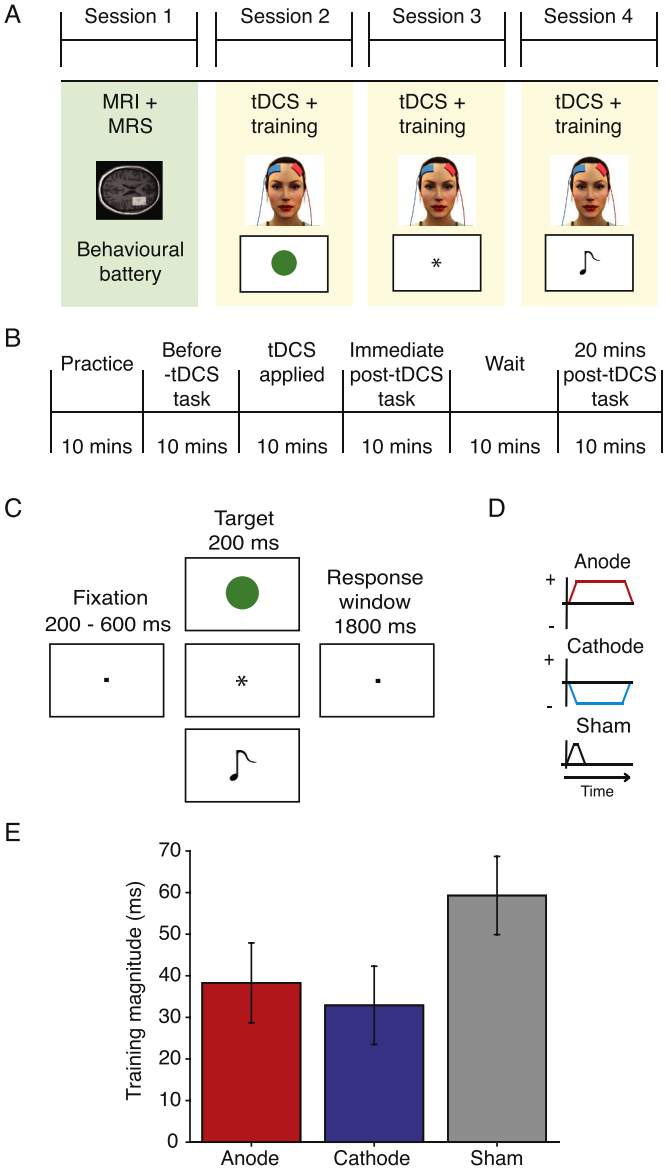

Fig. 1. Experiment overview. (A) Subjects each completed four sessions, one with MRI measures and a battery of behavioural tasks, and three with tDCS applied part way through learning a simple decision-making task. (B) For the tDCS sessions, subjects completed the task before, immediately after, and 20 min after application of stimulation. (C) The decision-making paradigm consisted of a simple fixation, followed by a stimulus (coloured circle, symbol, or sound), then a response window. (D) In each of the three stimulation sessions, subjects were given a different type of tDCS to the left prefrontal cortex: anodal, cathodal, and sham. (E) The magnitude of training benefits for the stimulation sessions, calculated as the difference from pre-to 20 min after tDCS (for correct trials). Error bars reflect the SEM for the change in response time from pre-to delayed post-tDCS.

2.2. Subjects

Fifty-five subjects took part in the study, of which eight were excluded: two for missing data, two for issues with the MRI scans, and four for poor performance at baseline (<70% accuracy for the key decision-making task, and/or particularly long response times (>3 SD from the mean)). The exclusion criteria were decided *a priori*. The subjects all passed a safety screening for both the MRI and the tDCS components of the study, and gave informed consent. The University of Queensland Human Research Ethics Committee approved the study.

2.3. Tasks

The study used a simple perceptual decision-making paradigm where subjects had to make speeded responses to visual or auditory stimuli (see Fig. 1C; also see Filmer et al., 2013a, 2013b). For each of the three stimulation sessions, subjects learned a new set of stimulus-response mappings. In one session, the stimuli consisted of a set of coloured circles (in RGB – red: 237 32 36, dark green: 10 130 65, dark blue: 44 71 151, light green: 109 205 119, light blue: 79 188 220, brown: 167 106 48, pink: 255 57 255, yellow: 255 235 30). In another session, a set of symbols was used (#, %, @, ~, ^, *, +, |), and in a third session a set of complex tones was presented (as used by Dux et al., 2006). The order of the stimulation sessions, and the pairing of stimulus sets with stimulation type (and session order) were counterbalanced across subjects. Each stimulus was associated with a separate key on the keyboard (A,S,D,F,H,J,K,L). For each session, subjects initially completed practice trials to learn the stimulus-response mappings. For example, they might have learned that if they saw a green circle, they had to press the 'A' key on the keyboard, whereas if they saw a red circle, they had to press the 'S' key, etc. At the start of the practice, they were initially shown the mappings (e.g. the colours were presented with the corresponding key listed above). They then completed practice blocks with feedback to learn the correct discriminations.

There were blocks in which two possible stimuli could be presented (low load), and blocks in which six possible stimuli could be presented (high load). We have previously shown that stimulation predominantly affects high-load performance (Filmer et al., 2013a, 2013b), and thus we focused on this condition for our analyses. After practice, an "offline" tDCS protocol was employed: a 'pre-tDCS' phase of the task was completed followed by the application of stimulation at rest. After the cessation of stimulation, the task was completed again (immediately--post tDCS). Following this there was a 10-min break, before the task was undertaken for a final time (delayed-post tDCS). Each phase of the experiment consisted of three blocks of 30 trials for each load (total of 180 trials), with the block types alternated. Half of the subjects started with a high load, and half with a low load. Subjects were instructed to respond as quickly and accurately as possible. In line with our previous work (Filmer et al., 2013a, 2013b), of which this was in part a replication, the main measure of interest was how subjects' performance changed with training – i.e., how much improvement there was from the pre-to the delayed-post timepoints.

2.4. MRI session

Brain imaging data were acquired using a 3 T Siemens Magnetom PRISMA scanner (Siemens Healthcare, Erlangen, Germany) fitted with a 64-channel head and neck coil. For the structural MRI, T1-weighted magnetization-prepared rapid gradient-echo (MPRAGE) images were acquired (TR: 1900 ms, TE: 2.26 ms, FA: 9°, FOV: 256 mm, voxel size: 1 mm isotropic). The T1 scans were analysed in Freesurfer version 6.0, using the standard Recon-All pipeline (Fischl et al., 2002). To avoid errors with the skull strip stage of the reconstruction, we performed a parallel skull strip using ROBEX (Iglesias et al., 2011), which then replaced the brain mask in Freesurfer before the autorecon2 stage. After the Freesurfer analyses, we extracted mean cortical thickness values for each subject in regions of interest proximal to the area targeted with tDCS (prefrontal cortex) based on ROIs available in the Destrieux atlas (Destrieux et al., 2010). The regions were the opercular and triangular regions of the inferior frontal gyrus, the middle frontal gryus, the inferior frontal sulcus, the middle frontal sulcus, and the inferior portion of the precentral sulcus. We focused our analyses on the left hemisphere and included the right hemisphere homologues as control regions. The location of key cortical regions are shown in Fig. 2A.

For the MRS, GABA+ and glutamate concentrations were estimated in the left prefrontal cortex for a volume 25 × 40 × 30 mm in size. The size of the volume is relatively large due to the poor signal-to-noise ratio for measuring neurochemicals, and is typical in the literature (e.g. Ghisleni et al., 2015; Michels et al., 2012). The location of the volume was selected in each subject using the following procedure: positioned on a slice 1.5 mm above the superior margin of the lateral ventricles, with the centre of the volume placed one third of the total anterior/posterior distance, centred halfway between the left lateral border and the midline (Ghisleni et al., 2015; Michels et al., 2012), and then adjusted as necessary to avoid CFS and dura/skull. Neurochemical concentrations were also estimated for the visual cortex, to act as a control region. This location was placed bilaterally over the calcarine fissure, again adjusted in each individual to avoid skull/dura/ventricles. The locations of the two MRS volumes are shown in Fig. 2B and C.

Outer volume suppression pulses were used to reduce signal

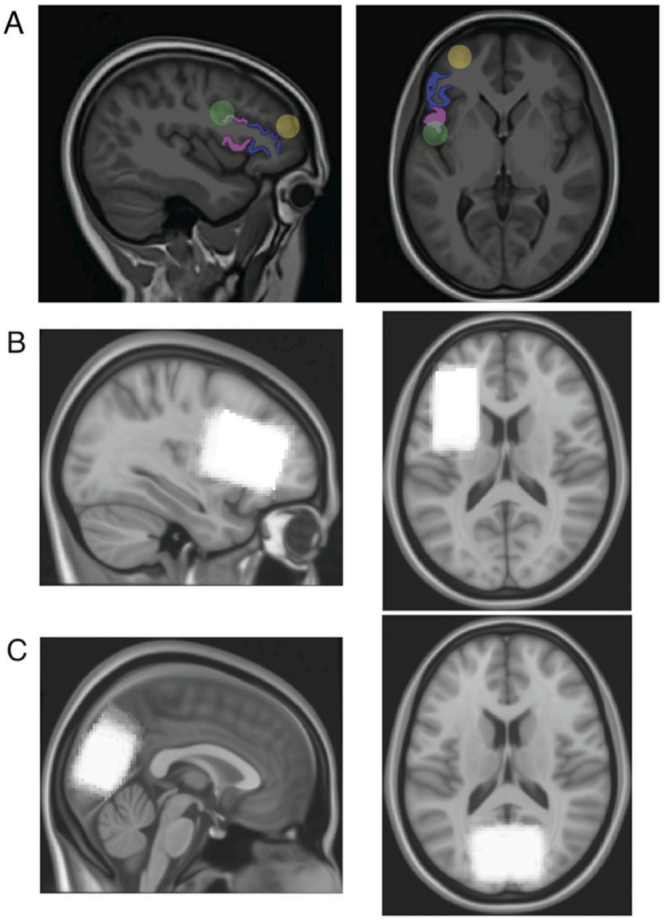

Fig. 2. Baseline measures of cortical morphology and neurochemicals. (A) Key regions of cortical morphology: triangular (blue) and opercular (pink) portions of the inferior frontal gyrus, the middle frontal sulcus (yellow) and the inferior precentral sulcus (green). The locations of the left prefrontal (B) and visual cortex (C) MRS volumes, plotted (overlapped, in partial transparency) for all subjects. (For interpretation of the references to colour in this figure legend, the reader is referred to the Web version of this article.)

contribution from outside the volume of interest. The volume was first shimmed, and then the following scan sequences were run: MEGA-PRESS (Mescher et al., 1998; Mescher et al., 1996; TR = 2000 ms, TE = 68 ms, 144 pairs of averages, ON editing pulse at 1.9 ppm, OFF editing pulse at 7.5 ppm) to assess for GABA+, PRESS sequence (TR = 2000 ms, TE = 30 ms, 128 averages) to assess for glutamate, and a complete phase cycle of measurements was acquired without the water suppression RF pulses to record a water peak reference for eddy current correction (Klose, 1990). The concentrations of GABA+ were extracted using the Gannet toolbox for Matlab (Edden et al., 2014), and glutamate was extracted using LCModel (Provencher, 1993). Both neurochemicals were estimated relative to concentrations of creatine. During the MRI session, subjects also completed a series of behavioural tasks as described in Filmer et al. (2019a, 2019b). The data from those tasks are included in the present study.

All subjects completed the MRI session one day before they started the tDCS sessions. Due to issues with the MRS scans, however, the first 11 subjects had to return and be re-scanned at a later date. MRS concentrations have been shown to be stable over a timeframe of months (Greenhouse et al., 2016; Near et al., 2014), and we have previously shown that accounting for the difference in scan timing in our analyses does not influence our findings (Filmer et al., 2019a, 2019b).

2.5. tDCS sessions

tDCS was delivered via a NeuroConn stimulation device, using soaked sponge electrodes. The target electrode (5 × 5 cm) was placed over the left prefrontal cortex (1 cm posterior to the 10–20 EEG location of F3). The reference electrode (5 × 7 cm) was placed over the right prefrontal cortex (1 cm posterior to F4). For all three stimulation conditions the current was ramped up/down over 30 s to 0.7 mA. For the two active stimulation conditions, the current was held constant for 8 min, and for the sham stimulation condition the current was held constant for 15 s. For one active condition the anode was placed over left prefrontal cortex and the cathode over right prefrontal cortex, and for the other condition this arrangement was reversed.

2.6. Modelling

The LBA parameters were estimated from the accuracy and response time data from the decision-making task, using the LBA model (see Fig. 3 for a schematic representation). This model assumes that evidence for each response alternative accumulates independently in separate accumulators. There were six response alternatives in this experiment, so the model included six evidence accumulators. The amount of evidence for each alternative at the start of each decision trial is drawn from a uniform distribution on the interval $[0, A]$, where A represent the maximum starting point of evidence accumulation. The evidence then accumulates linearly. For each accumulator, the rate at which evidence accumulates (the drift rate) is drawn from a normal distribution with mean v and standard deviation sv. Evidence accumulates until the evidence for one alternative reaches a threshold (b), at which point that alternative is selected and the response is made. As is common practice (e.g., Brown and Heathcote, 2008), we express threshold in terms of the difference between the raw threshold and the maximum starting point for evidence (denoted B, where $B = b - A$). The LBA also includes a non-decision time parameter (t_0) that captures the component of the response time attributable to processes other than the decision process (e.g., encoding the stimulus and manually executing the response).

The mean rate of evidence accumulation for the correct response was allowed to vary as a function of time (pre-versus delayed-post tDCS) and stimulation type (anodal, cathodal, or sham). The mean rate for the incorrect response was constrained to be equal across conditions, as the low rate of errors would have made it difficult to estimate separate rates for the incorrect accumulator in each condition. Threshold and non-decision time were allowed to vary across time and stimulation conditions. Starting point variability was constrained to be equal across conditions. In order to make the model identifiable, we fixed the standard deviation of the rate of evidence accumulation to one for all accumulators in all conditions.

We estimated these parameters using a hierarchical Bayesian framework (Boehm et al., 2018; Rouder and Lu, 2005), which assumed that parameters varied across individuals, but were drawn from common population distributions. The population distribution for each parameter required two hyperparameters: location and scale (see Table 1). The subject-level parameters were modelled using normal or truncated normal distributions. The A and B parameters each had a lower bound of 0 and no upper bound. The t_0 parameter had a lower bound of 0.05 and an upper bound of 1. The v parameter was not truncated.

The posterior distributions were estimated using the differential evolution MCMC algorithm (Turner Sederberg et al., 2013), as implemented by the DMC package (Heathcote et al., 2019) in R. For each model, we ran 60 chains, which was three times the number of subject-level parameters (the DMC package default). We used a thinning interval of 10, meaning that one sample was saved every 10 iterations. Sampling was done using the auto-convergence routine enabled by the 'run.unstuck.dmc' and 'run.converge.dmc' functions, which sample until the multivariate potential scale reduction factor is less than 1.1 for all subjects. At this point, we discarded all previous samples and

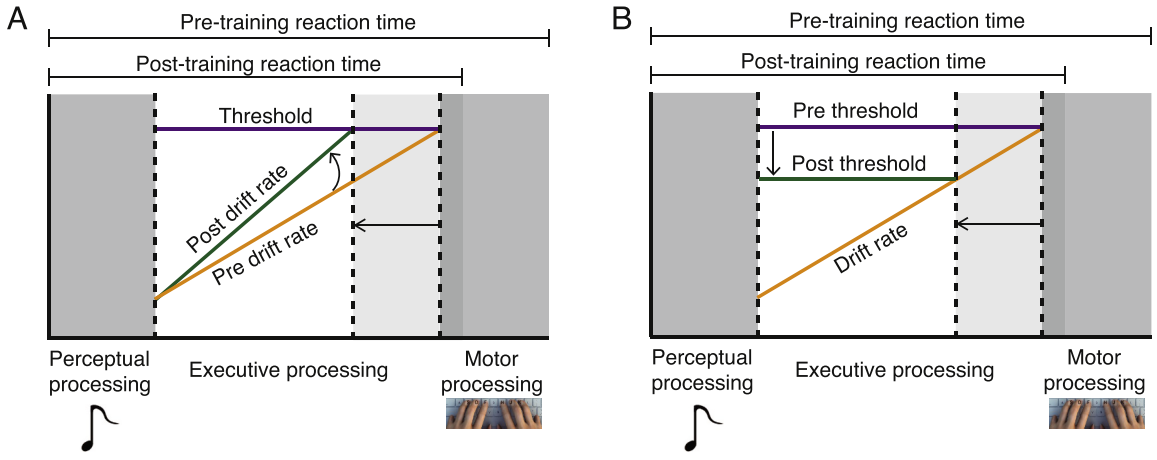

Fig. 3. Schematic depiction of latent decision variables and how they may change with training. Faster responses typically seen with training may increase the drift rate (A), and/or reduce the response threshold (B).

Table 1
Priors on Population-level Parameters of the LBA.

Population Distribution	Model Parameter	Distribution Family	Mean	SD	Lower	Upper
Location	*A*	Truncated Normal	1	5	0	None
	B	Truncated Normal	1	5	0	None
	V	Normal	1	5	None	None
	t_0	Truncated Normal	0.3	1	0.05	1
Scale	*A*	Truncated Normal	0	2	0	None
	B	Truncated Normal	0	2	0	None
	v	Truncated Normal	0	2	0	None
	t_0	Truncated Normal	0	1	0	None

collected a fresh 1000 samples per chain. This resulted in a total of 60 000 samples per parameter (1000 samples x 60 chains). Visual inspection of the final chains showed excellent mixing and stationarity.

Fig. 4A shows the observed proportion of responses and the proportions predicted by the model for each condition. Fig. 4B shows the observed and predicted distribution of response times. The observed values in each plot were calculated by first obtaining the relevant value (the response proportion or response time quantile for a particular condition) for each subject, and then taking the average of that value across subjects. The predicted values were calculated by repeating the above procedure for each sample, so that the full posterior distribution could be obtained for each value. As can be seen in Fig. 4, the model provides a fairly close fit to accuracy data and the distribution of correct response times. The fit of the model to the incorrect response time distribution was less accurate. However, because of the low error rate, the incorrect responses provided less information to constrain the parameter estimates than the correct responses (Donkin et al., 2011). Thus, it is not surprising that the model-data alignment was weaker for the incorrect response time distribution compared with the correct response time distribution.

2.7. Analyses

Computation of variables. The key variables of interest were the changes in each component of the decision process across training sessions – i.e., changes in the difference in mean drift rate between correct and incorrect evidence accumulators (i.e., changes in discriminability), threshold, and non-decision time from pre-to delayed-post tDCS time points. These change variables were generated for each stimulation type by subtracting the parameter estimate associated with the pre-test from the estimate associated with the delayed-post-test (resulting in a variable representing performance change with learning). We then calculated the effect of stimulation for each polarity compared with sham, through subtraction (i.e., the amount of learning under the sham condition minus that under the anodal condition, and the amount of learning for the sham condition minus that for the cathodal condition). The effect of each polarity was calculated in this manner for the drift rates, thresholds, and non-decision times. The variables used in the analyses were the mean of the posterior distribution on the relevant polarity effect.

Variability. Individual differences were assessed through the use of Bayesian linear regressions (JASP Team, 2017). The effect of each active stimulation condition on learning (relative to sham) were entered in turn as dependent variables for each of the three latent components estimated from the LBA. Independent variables were GABA+/Cr, glutamate/Cr, the ratio of GABA + to glutamate, and cortical thickness in the following regions: opercular, triangular, and middle gyri and the middle frontal, inferior precentral, and the inferior frontal sulci. The analyses employed a relatively large null model to account for other sources of variability, including age, sex, the pairing of stimulus set with stimulation condition, grey and white matter fractions of the MRS volume of interest, and the two latent components not entered as the dependent variable (e.g., if the drift rate difference was the dependent variable, threshold and non-decision time were included in the null model). This was done to assess for the *unique* variance explained by each component. The 'winning' model (highest BF_{10} value) from each analysis was selected and reported.

2.8. Interpretation

For Bayes factors for the alternative hypothesis (BF_{10}), values of ~1 were treated as non-evidential, 1–3 as weak evidence, 3–10 as moderate evidence, and over 10 as strong evidence. The same interpretation was

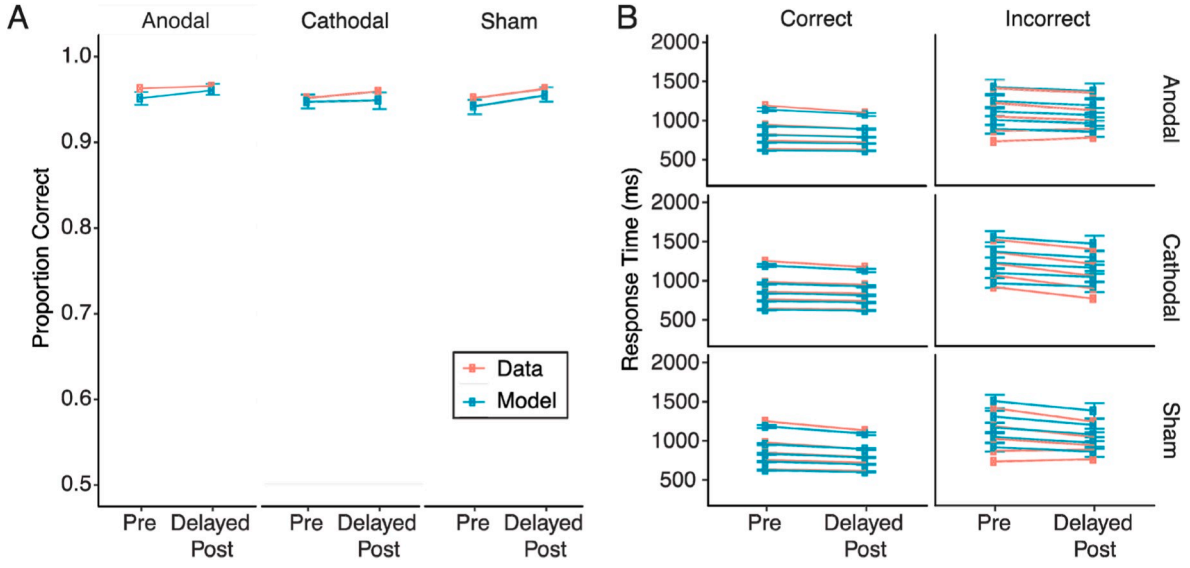

Fig. 4. Actual data and model fits for the accuracy data (A) and response times (B). The five sets of lines for the model and data shown in (B) represent the means of the 10th, 30th, 50th, 70th, and 90th percentiles of the response time distribution.

given for Bayes factors in favour of the null (BF_{01}). Credible intervals (95%; CIs) were used to interpret the group-level effects of stimulation on the latent components. We inferred credible effects if the CI on the average effect excluded 0.

2.9. Data availability

The materials used to run the study and extract the task data, the behavioural, MRI, and MRS data are all publicly available (Filmer et al., 2019a, 2019b).

3. Results

3.1. Group level effects of stimulation on response times

Analyses of the response time data have been reported previously (Filmer et al., 2019a; Filmer et al., 2019b). We first assessed baseline (pre-stimulation) response times to ensure any differences between the stimulation conditions were not driven by differences in the starting points. Paired t-tests revealed no evidence for differences between the three stimulation conditions ($BF_{01} > 2.9$, $p > 0.2$, for all).

Both anodal and cathodal stimulation disrupted training related gains present for sham tDCS (see Fig. 1E). Compared with sham stimulation, the effect of cathodal stimulation was reliable ($BF_{10} = 3.446$), but the effect of anodal stimulation was weak ($BF_{10} = 1.347$).

3.2. Group level effects of stimulation on latent variables

Group-level assessment of stimulation modulations of the drift rate difference, threshold, and non-decision time are depicted in Fig. 5. Under sham stimulation, training led to an increase in drift rates [CI: 0.204, 0.4], a decrease in threshold [CI:−0.219, −0.031], and a small increase in non-decision time [CI: 0.015, 0.06]. Thus, in the absence of active stimulation, training increased the rate at which evidence was accumulated, decreased caution, and led to slight increases in the rate of sensory/motor processing.

There appeared to be no meaningful difference between training related changes for the cathodal relative to sham session on threshold [CI: −0.155, 0.102] or non-decision time [CI cathodal vs. sham: −0.022, 0.025]. However, there was less of an increase in the drift rate under cathodal stimulation relative to sham [CI: −0.275, −0.006]. There was no meaningful difference between training related changes for the anodal relative to sham session on drift rate [CI anodal vs. sham: −0.116, 0.168] or non-decision time [CI anodal vs. sham: −0.035, 0.014]. However, there was a borderline effect for less of a reduction in threshold for anode relative to sham [CI anodal vs. sham: −0.012, 0.27]. Thus, at the group level, there may be a tendency for anodal stimulation to lead to a reduction in performance gains via a modulation of response threshold, whereas cathodal stimulation led to attenuated improvements in the rate at which evidence was accumulated in the decision-making task.

3.3. Accounting for variability in stimulation efficacy

Anodal stimulation. The effect of anodal stimulation (relative to sham) was related to cortical thickness in the opercular and triangular gyri, and the middle frontal sulcus, for all three parameters of the LBA model, including the drift rate difference ($BF_{10} = 22.633$, $R^2 = 0.707$), threshold ($BF_{10} = 9.886$, $R^2 = 0.867$), and non-decision time ($BF_{10} = 22.407$, $R^2 = 0.827$; see Fig. 6). Thus, the efficacy of anodal stimulation in modulating the three latent components was related to the same three cortical regions in the inferior frontal gyrus and middle frontal sulcus (not to the middle gyrus, or inferior precentral or inferior frontal sulci).

Cathodal stimulation. The effect of cathodal stimulation (relative to sham) on the drift rate difference was related to the relative concentrations of GABA+ and glutamate (the ratio of neurochemical excitability) and cortical thickness in the inferior precentral sulcus ($BF_{10} = 5.455$, $R^2 = 0.727$; see Fig. 7). None of the included independent variables could account for variability in the effect of cathodal stimulation on thresholds or non-decision time ($BF_{10} < 1$ for all). To sum, variability in the efficacy of cathodal stimulation related to a combination of cortical thickness and neurochemical variables, but only in reference to the drift rate component of decision-making.

3.4. Control analyses

A set of linear regressions were run to control for the potential influence of extraneous variables on the analyses above, following the same approach, but for MRS data derived from the visual cortex (which served as a control region) and for right hemisphere cortical thickness (again as a control for the homologous left hemisphere regions assessed above). These control analyses – which assessed the effect of anodal and cathodal tDCS, relative to sham, on the drift rate difference, threshold, and non-decision time with the same null models as the key analyses above – yielded limited evidence for all relationships ($BF_{10} < 2.4$) with one exception: variability in anodal stimulation modulation of drift rates was related to cortical thickness in the right hemisphere middle frontal and inferior precentral sulci, the concentration of glutamate in the visual cortex, and the relative concentration of GABA + to glutamate in the visual cortex ($BF_{10} = 19.017$, $R^2 = 0.752$). Of importance, however, there were correlations between the left and right hemisphere cortical thickness for the middle frontal sulci ($r = 0.33$, CI: 0.04, 0.55), and the inferior precentral sulci ($r = 0.3$, CI: 0.014, 0.53), and also between the left prefrontal and visual cortices for glutamate concentrations ($r = 0.44$, CI: 0.17, 0.63), and the ratio of neurochemical excitability ($r = 0.3$, CI: 0.007, 0.53). Thus, collectively, while this model explained a

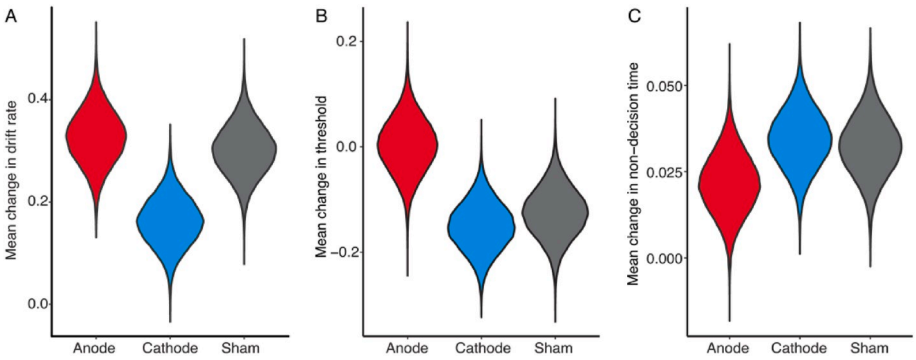

Fig. 5. Violin plots depicting the group-level effects of training and stimulation on latent response components. (A) Sham and anodal stimulation conditions result in increased drift rates, which are attenuated with cathodal stimulation. (B) Sham and cathodal stimulation conditions lead to a decrease in response threshold which is attenuated by anodal stimulation. (C) All three stimulation conditions show a small increase in non-decision time.

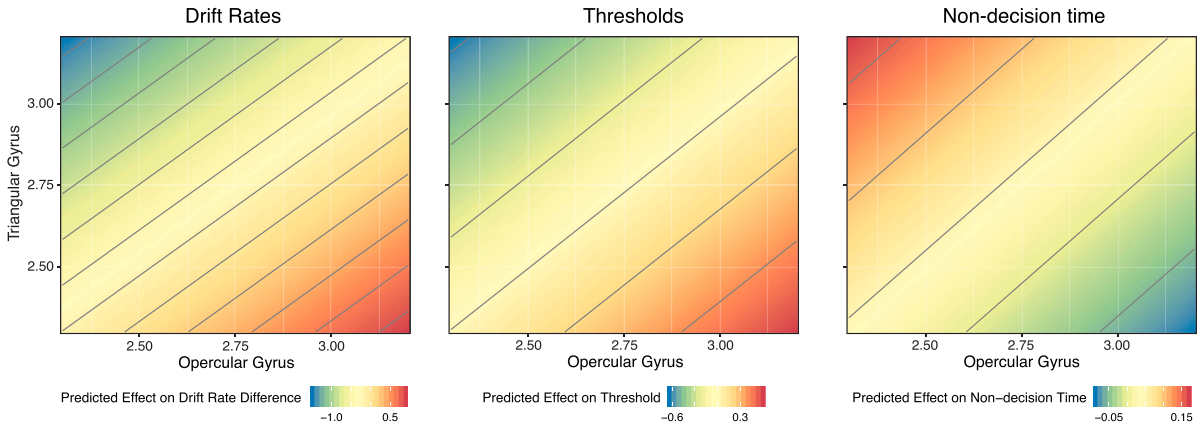

Fig. 6. Surface plots depicting the relationship between disruption to training-related improvements in the drift rate difference (left), threshold (centre), and non-decision time (right) from anodal tDCS and two of the key independent variables: cortical thickness in the opercular (x-axis) and triangular (y-axis) gyri.

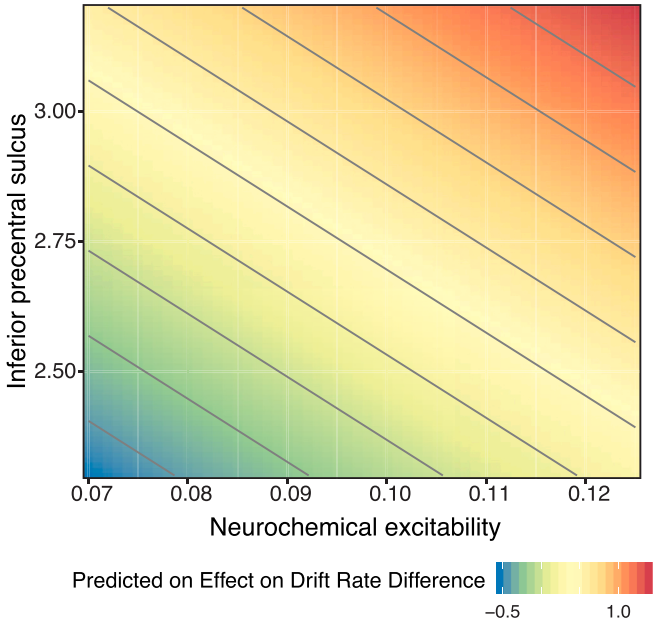

Fig. 7. Surface plot depicting the relationship between disruption to training-related improvements in drift rates from cathodal tDCS and two key independent variables: the ratio of GABA + to glutamate (neurochemical excitability) and cortical thickness in the inferior precentral sulcus.

meaningful amount of the data, this finding is difficult to interpret as it reflects a relatively complex model, does not fit with any expectations or hypotheses, and may relate to the strong correlations with the key measures of interest.

To assess whether individual differences in the induced current in the cortex could contribute to our results, we ran the critical regressions again but included the estimated (medium) current in the inferior frontal gyrus (our target region). Induced current (V/m) was estimated using ROAST (Huang et al., 2018) in individual subject space. ROAST applies conductance values for each tissue type, specifically (units in S m^{-1}): grey matter 0.276, white matter 0.126, CFS 1.65, skull 0.01, scalp 0.465. For each individual, values for two 5 × 5 × 5 mm volumes – the opercular and triangular portions of the inferior frontal gyrus – were extracted and the median values were calculated to give an estimation of the induced current for each of these two regions. At a group level, these values were 0.049 V/m (SD 0.009) and 0.044 V/m (SD 0.012) for the opercular and triangular regions, respectively. Including these two values for each subject in the regressions did not change the pattern of results, with the effect of cathodal tDCS on drift rates relating to cortical thickness in the precentral sulcus and the ratio of GABA to glutamate (BF_{10} = 4.67). For anodal stimulation, individual differences remained related to the opercular and triangular gyri, and the middle frontal sulcus for thresholds (BF_{10} = 6.68), drift rates (BF_{10} = 17.42), and non-decision time (BF_{10} = 17.8).

4. Discussion

Here we combined tDCS over the prefrontal cortex with a behavioural task, brain imaging and computational modelling to understand the latent processes associated with simple decision-making and how these are influenced by brain stimulation. We replicated our previous behavioural findings (Filmer et al., 2013a, 2013b; Filmer et al., 2013a, 2013b), namely, that offline prefrontal tDCS disrupts learning on a simple decision-making task. Crucially, through the use of computational modelling, we found that disruption of behavioural training effects via cathodal or anodal tDCS reflect changes in distinct underlying processes. Specifically, at a group-level, cathodal stimulation disrupted training gains by hindering improvements in the ability to discriminate between correct and incorrect responses, whereas there was a tendency for anodal stimulation to disrupt training gains by counteracting a decrease in response threshold. Moreover, variability in the effects of the two polarities of stimulation on behaviour was associated with differences in two distinct neurophysiological measures. Thus, despite the apparent similarities in the effect of anodal and cathodal tDCS on response times in our decision-making task, the two polarities of stimulation are in fact dissociable in terms of the latent decision components and related neurophysiological factors.

In previous work we have shown that disruption of decision-making training with offline tDCS is specific to targeting the left prefrontal cortex. No such modulation occurs with the right prefrontal cortex (Filmer et al., 2013a, 2013b); nor is the effect dependent upon the location of the reference electrode (Filmer et al., 2013a, 2013b). Our findings complement previous imaging studies that reported performance improvement with training is specifically associated with a region of the left prefrontal cortex (the inferior frontal junction; Dux et al., 2009), and have now been replicated multiple times (Filmer et al., 2013a, 2013b; Filmer et al., 2013a, 2013b).

Previous reports have suggested that anodal and cathodal tDCS can have opposing effects, for example by increasing and decreasing cortical excitability (e.g. Nitsche and Paulus, 2000b). This may be related to reductions in two separate neurochemicals: GABA (inhibitory) with anodal stimulation (Bachtiar et al., 2018; Bachtiar, et al., 2015; Stagg

et al., 2009; Stagg et al., 2011), and glutamate (excitatory) with cathodal stimulation (Stagg et al., 2009). However, it is likely that the two polarities have a more complex effect on the underlying cortex, with varying effects due to factors such as the orientation of neurons relative to the induced current (Liu et al., 2018; Rawji et al., 2018), differences in outcomes depending on stimulation intensity/duration (Samani et al., 2019), and considerable individual variability in the extent (and even direction) of modulations (Wiethoff et al., 2014, although see van de Ruit and Grey, 2019). Given our previous findings of polarity non-specific performance modulation (on reaction times) in a decision-making task, we had hypothesised that decision-making training may be achieved via a finely tuned system in the left prefrontal cortex (Filmer et al., 2013a, 2013b). Any disruption to this system – either excitatory or inhibitory, from either anodal or cathodal stimulation – can result in a disruption to training related performance gains. Given our findings here, we can now update this hypothesis and suggest that each polarity affects a different decision component. If we can further elucidate how each stimulation polarity modulates neural function, we may in the future be able to go further and infer the properties of systems differentially affected by the two polarities of stimulation.

Our findings do not specifically relate to how the cortex changes with stimulation, however it appears that any offline effects of the two polarities are influenced by separable neurophysiological measures at baseline relating to distinct neural architecture and neurochemicals. Variation in the efficacy of cathodal stimulation appears to relate to the relative neurochemical excitability of the prefrontal cortex, and to cortical thickness in one posterior part of the same region (the inferior precentral sulcus). In contrast, no relationship was apparent between anodal stimulation and neurochemical concentrations, and the three brain regions whose cortical thickness predicted efficacy (opercular and triangular gyri, and middle frontal sulcus) were separate (albeit neighbouring) to the region implicated in cathodal efficacy.

Not only were there dissociations in the region(s) and neurochemical relationships, but variations in the efficacy of cathodal stimulation were more specific (relating only to the difference in drift rate) than for anodal stimulation, where efficacy related to cortical structure for all three of the latent variables modelled. In our analyses we examined the unique variance related to each latent variable in turn. For example, when considering the drift rate difference as the dependent variable, thresholds and non-decision times were entered into the null model. Thus, the efficacy of anodal stimulation to modulate the drift rate difference, threshold, and non-decision time appears to independently relate to cortical thickness in the three identified regions. In other words, it is relatively unlikely that there is a shared or underlying factor present in all three latent variables. For cathodal stimulation, variability in the effect on the drift rate difference was only related to baseline neurophysiology, and thus shows a much more specific relationship. Overall, then, it appears that the efficacy of the two stimulation polarities to modulate behaviour, when applied to the same brain region, relate to different decision processes and also different neurophysiological measures/systems in the frontal cortex.

The relationship between cortical thickness and stimulation efficacy could relate to two separate (although not mutually exclusive) factors. First, cortical thickness may directly influence current flow. There are known differences in resistivity between grey matter, white matter and CSF, and the path of least resistance likely varies depending on the exact topology of different individuals with varying thicknesses (Alekseichuk et al., 2019) – with thicker/thinner cortical grey matter affecting the channelling of the current and resulting in areas being affected to varying degrees by stimulation. Alternatively, cortical thickness might itself relate to task performance (e.g., Bi et al., 2014), and thus how susceptible the individual subject is to modulations to performance with stimulation. For the MRS data, as we accounted for the *amount* of grey (and white) matter in the volume recorded from our regression analyses, the individual and relative concentrations of GABA+ and glutamate are unlikely to relate to the cortical thickness data. As shown in Fig. 2, the region from which neurochemicals were recorded was relatively large, and encompassed regions included in the cortical thickness analyses (e.g. the inferior frontal gyrus).

Here we have provided the first evidence for a combined role of neurochemicals and cortical morphology in individual variability in the response to tDCS. The use of individual differences to link brain structure (Frank et al., 2016; Kanai et al., 2010; Verghese et al., 2016), function (Drew and Vogel, 2008; Garner and Dux, 2015), and neurochemical concentrations (Terhune et al., 2014; Yoon et al., 2016) to behaviour illustrates that there is important information across individuals that is lost when averaging across groups. In the context of the study we report here, the use of individual differences and neuroimaging can advance understanding of the key factors that relate to, and may in the future predict, the efficacy of stimulation on behaviour. This could shed light not only on the mechanisms of brain stimulation, but might also help in the development of the most effective protocols for treating relevant clinical conditions.

CRediT authorship contribution statement

Hannah L. Filmer: Formal analysis, Methodology, Data curation, Writing - original draft, Writing - review & editing. **Timothy Ballard:** Formal analysis, Writing - review & editing. **Shane E. Ehrhardt:** Methodology, Data curation, Writing - review & editing. **Saskia Bollmann:** Formal analysis, Writing - review & editing. **Thomas B. Shaw:** Formal analysis, Writing - review & editing. **Jason B. Mattingley:** Funding acquisition, Methodology, Writing - review & editing. **Paul E. Dux:** Funding acquisition, Methodology, Writing - review & editing.

Acknowledgements

This research was supported by an Australian Research Council (ARC) Discovery grant (DP140100266, PED & JBM), the ARC-SRI Science of Learning Research Centre (SR120300015, PED & JBM), and the ARC Centre of Excellence for Integrative Brain Function (ARC Centre Grant CE140100007, JBM). JBM was supported by an ARC Australian Laureate Fellowship (FL110100103), HLF by a UQ Fellowship (UQFEL1607881) and ARC Discovery Early Career Researcher Award (DE190100299), and TB by an ARC Discovery Early Career Researcher Award (DE180101340). SB acknowledges support through the Australian Government Research Training Program Scholarship. We thank Siemens for providing the MEGA-PRESS sequence, and Dr Desmond H. Y. Tse for his help with acquiring the MRS scans and analysing the data. We thank research radiographers, Mr Aiman Al Najjar and Ms Nicole Atcheson for their assistance in acquiring the MRI and MRS scans.

References

Alekseichuk, I., Mantell, K., Shirinpour, S., Opitz, A., 2019. Comparative modeling of transcranial magnetic and electric stimulation in mouse, monkey, and human. Neuroimage 194, 136–148. https://doi.org/10.1016/J.NEUROIMAGE.2019.03.044.

Bachtiar, V, Johnstone, A, Berrington, A, Lemke, C, Johansen-Berg, H, Emir, U, Stagg, CJ, 2018. Modulating regional motor cortical excitability with non-invasive brain stimulation results in neurochemical changes in bilateral motor cortices. J. Neurosci. 38 (33), 7327–7336. https://doi.org/10.1523/JNEUROSCI.2853-17.2018.

Bachtiar, V, Near, J, Johansen-Berg, H, Stagg, CJ, 2015. Modulation of GABA and resting state functional connectivity by transcranial direct current stimulation. ELife. https://doi.org/10.7554/eLife.08789.

Bi, T., Chen, J., Zhou, T., He, Y., Fang, F., 2014. Function and structure of human left fusiform cortex are closely associated with perceptual learning of faces. Curr. Biol. 24 (2), 222–227. https://doi.org/10.1016/J.CUB.2013.12.028.

Boehm, U., Marsman, M., Matzke, D., Wagenmakers, E.-J., 2018. On the importance of avoiding shortcuts in applying cognitive models to hierarchical data. Behav. Res. Methods 50 (4), 1614–1631. https://doi.org/10.3758/s13428-018-1054-3.

Brown, S.D., Heathcote, A., 2008. The simplest complete model of choice response time: linear ballistic accumulation. Cognit. Psychol. 57 (3), 153–178.

Brunoni, A.R., Moffa, A.H., Sampaio-Junior, B., Borrione, L., Moreno, M.L., Fernandes, R. A., Benseñor, I.M., 2017. Trial of electrical direct-current therapy versus escitalopram for depression. N. Engl. J. Med. 376 (26), 2523–2533. https://doi.org/10.1056/NEJMoa1612999.

Destrieux, C., Fischl, B., Dale, A., Halgren, E., 2010. Automatic parcellation of human cortical gyri and sulci using standard anatomical nomenclature. Neuroimage 53 (1), 1–15. https://doi.org/10.1016/j.neuroimage.2010.06.010.
Donkin, C., Brown, S., Heathcote, A., 2011. Drawing conclusions from choice response time models: a tutorial using the linear ballistic accumulator. J. Math. Psychol. 55 (2), 140–151.
Drew, T., Vogel, E.K., 2008. Neural measures of individual differences in selecting and tracking multiple moving objects. J. Neurosci.: Off. J. Soc. Neurosci. 28 (16), 4183–4191. https://doi.org/10.1523/JNEUROSCI.0556-08.2008.
Dux, P.E., Ivanoff, J., Asplund, C.L., Marois, R., 2006. Isolation of a central bottleneck of information processing with time-resolved fMRI. Neuron 52 (6), 1109–1120.
Dux, P.E., Tombu, M.N., Harrison, S., Rogers, B.P., Tong, F., Marois, R., 2009. Training improves multitasking performance by increasing the speed of information processing in human prefrontal cortex. Neuron 63 (1), 127–138.
Edden, R.A., Puts, N.A., Harris, A.D., Barker, P.B., Evans, C.J., 2014. Gannet: a batch-processing tool for the quantitative analysis of gamma-aminobutyric acid-edited MR spectroscopy spectra. J. Magn. Reson. Imag. 40 (6), 1445–1452. https://doi.org/10.1002/jmri.24478.
Filmer, H.L., Dux, P.E., Mattingley, J.B., 2014. Applications of transcranial direct current stimulation for understanding brain function. Trends Neurosci. 37 (12) https://doi.org/10.1016/j.tins.2014.08.003.
Filmer, H.L., Lyons, M., Mattingley, J.B., Dux, P.E., 2017a. Anodal tDCS applied during multitasking training leads to transferable performance gains. Sci. Rep. 7 (1) https://doi.org/10.1038/s41598-017-13075-y.
Filmer, H.L., Mattingley, J.B., Dux, P.E., 2013a. Improved multitasking following prefrontal tDCS. Cortex 49 (10). https://doi.org/10.1016/j.cortex.2013.08.015.
Filmer, H.L., Mattingley, J.B., Marois, R., Dux, P.E., 2013b. Disrupting prefrontal cortex prevents performance gains from sensory-motor training. J. Neurosci. 33 (47) https://doi.org/10.1523/JNEUROSCI.2019-13.2013.
Filmer, H.L., Varghese, E., Hawkins, G.E., Mattingley, J.B., Dux, P.E., 2017b. Improvements in attention and decision-making following combined behavioral training and brain stimulation. Cerebr. Cortex 27 (7). https://doi.org/10.1093/cercor/bhw189.
Filmer, Hannah L., Ehrhardt, S.E., Shaw, T.B., Mattingley, J.B., Dux, P.E., 2019a. The efficacy of transcranial direct current stimulation to prefrontal areas is related to underlying cortical morphology. Neuroimage 196, 41–48. https://doi.org/10.1016/J.NEUROIMAGE.2019.04.026.
Filmer, Hannah L., Ehrhardt, S., Bollmann, S., Mattingley, J.B., Dux, P.E., 2019b. Accounting for individual differences in the response to tDCS with baseline levels of neurochemical excitability. Cortex. https://doi.org/10.1016/j.cortex.2019.02.012.
Fischl, B., Salat, D.H., Busa, E., Albert, M., Dieterich, M., Haselgrove, C., et al., 2002. Whole brain segmentation: automated labeling of neuroanatomical structures in the human brain. Neuron 33 (3), 341–355. Retrieved from. http://www.ncbi.nlm.nih.gov/pubmed/11832223.
Frank, S.M., Reavis, E.A., Greenlee, M.W., Tse, P.U., 2016. Pretraining cortical thickness predicts subsequent perceptual learning rate in a visual search task. Cerebr. Cortex 26 (3), 1211–1220. https://doi.org/10.1093/cercor/bhu309.
Garner, K.G., Dux, P.E., 2015. Training conquers multitasking costs by dividing task representations in the frontoparietal-subcortical system. Proc. Natl. Acad. Sci. Unit. States Am. 112 (46), 14372–14377. https://doi.org/10.1073/pnas.1511423112.
Ghisleni, C., Bollmann, S., Poil, S.S., Brandeis, D., Martin, E., Michels, L., et al., 2015. Subcortical glutamate mediates the reduction of short-range functional connectivity with age in a developmental cohort. J. Neurosci. 35 (22), 8433–8441. https://doi.org/10.1523/jneurosci.4375-14.2015.
Greenhouse, I., Noah, S., Maddock, R.J., Ivry, R.B., 2016. Individual differences in GABA content are reliable but are not uniform across the human cortex. Neuroimage 139, 1–7. https://doi.org/10.1016/j.neuroimage.2016.06.007.
Heathcote, A., Lin, Y.-S., Reynolds, A., Strickland, L., Gretton, M., Matzke, D., 2019. Dynamic models of choice. Behav. Res. Methods 51 (2), 961–985. https://doi.org/10.3758/s13428-018-1067-y.
Huang, Y, Datta, A, Bikson, M, Parra, LC, 2018. ROAST: An open-source, fully-automated, realistic volumetric-approach-based simulator for TES. Conf Proc IEEE Eng Med Biol Soc. https://doi.org/10.1109/EMBC.2018.8513086.
Iglesias, J.E., Cheng-Yi Liu, C.-Y., Thompson, P.M., Zhuowen Tu, Z., 2011. Robust brain extraction across datasets and comparison with publicly available methods. IEEE Trans. Med. Imag. 30 (9), 1617–1634. https://doi.org/10.1109/TMI.2011.2138152.
Kanai, R., Bahrami, B., Rees, G., 2010. Human parietal cortex structure predicts individual differences in perceptual rivalry. Curr. Biol.: CB 20 (18), 1626–1630. https://doi.org/10.1016/j.cub.2010.07.027.
Klose, U., 1990. In vivo proton spectroscopy in presence of eddy currents. Magn. Reson. Med. 14 (1), 26–30.
Liu, A., Vöröslakos, M., Kronberg, G., Henin, S., Krause, M.R., Huang, Y., et al., 2018. Immediate neurophysiological effects of transcranial electrical stimulation. Nat. Commun. 9 (1), 5092. https://doi.org/10.1038/s41467-018-07233-7.
Mescher, M., Merkle, H., Kirsch, J., Garwood, M., Gruetter, R., 1998. Simultaneous in vivo spectral editing and water suppression. NMR Biomed. 11, 266–272. EPFL-ARTICLE-177509.
Mescher, M., Tannus, A., Johnson, M., Garwood, M., 1996. Solvent suppression using selective echo dephasing. J. Magn. Reson., Ser. A 123 (2), 226–229.
Michels, L., Martin, E., Klaver, P., Edden, R., Zelaya, F., Lythgoe, D.J., et al., 2012. Frontal GABA levels change during working memory. PloS One 7 (4), e31933. https://doi.org/10.1371/journal.pone.0031933.
Near, J., Ho, Y.-C.L., Sandberg, K., Kumaragamage, C., Blicher, J.U., 2014. Long-term reproducibility of GABA magnetic resonance spectroscopy. Neuroimage 99 (Suppl. C), 191–196. https://doi.org/10.1016/j.neuroimage.2014.05.059.
Nitsche, M.A., Paulus, W., 2000a. Excitability changes induced in the human motor cortex by weak transcranial direct current stimulation. J. Physiol. 527 (3), 633–639. https://doi.org/10.1111/j.1469-7793.2000.t01-1-00633.x.
Nitsche, M.A., Paulus, W., 2000b. Excitability changes induced in the human motor cortex by weak transcranial direct current stimulation. J. Physiol. 527 (3), 633–639. https://doi.org/10.1111/j.1469-7793.2000.t01-1-00633.x.
Nord, C.L., Chamith Halahakoon, D., Limbachya, T., Charpentier, C., Lally, N., Walsh, V., et al., 2019. Neural predictors of treatment response to brain stimulation and psychological therapy in depression: a double-blind randomized controlled trial. Neuropsychopharmacology 1. https://doi.org/10.1038/s41386-019-0401-0.
Parkin, B.L., Ekhtiari, H., Walsh, V.F., 2015, September 2. Non-invasive human brain stimulation in cognitive neuroscience: a primer. Neuron. Elsevier. https://doi.org/10.1016/j.neuron.2015.07.032.
Provencher, S.W., 1993. Estimation of metabolite concentrations from localized in vivo proton NMR spectra. Magn. Reson. Med. 30 (6), 672–679.
Rawji, V., Ciocca, M., Zacharia, A., Soares, D., Truong, D., Bikson, M., et al., 2018. tDCS changes in motor excitability are specific to orientation of current flow. Brain Stimul. 11 (2), 289–298. https://doi.org/10.1016/J.BRS.2017.11.001.
Roberts, A.C., Robbins, T.W., Weiskrantz, L.E., 1998. The Prefrontal Cortex: Executive and Cognitive Functions. Oxford University Press.
Rouder, J.N., Lu, J., 2005. An introduction to Bayesian hierarchical models with an application in the theory of signal detection. Psychon. Bull. Rev. 12 (4), 573–604. https://doi.org/10.3758/BF03196750.
Samani, M.M., Agboada, D., Jamil, A., Kuo, M.-F., Nitsche, M.A., 2019. Titrating the neuroplastic effects of cathodal transcranial direct current stimulation (tDCS) over the primary motor cortex. Cortex. https://doi.org/10.1016/J.CORTEX.2019.04.016.
Stagg, C.J., Best, J.G., Stephenson, M.C., O'Shea, J., Wylezinska, M., Kincses, Z.T., et al., 2009. Polarity-sensitive modulation of cortical neurotransmitters by transcranial stimulation. J. Neurosci. 29 (16), 5202–5206. https://doi.org/10.1523/JNEUROSCI.4432-08.2009.
Stagg, C.J., Jayaram, G., Pastor, D., Kincses, Z.T., Matthews, P.M., Johansen-Berg, H., 2011. Polarity and timing-dependent effects of transcranial direct current stimulation in explicit motor learning. Neuropsychologia 49, 800–804. https://doi.org/10.1016/j.neuropsychologia.2011.02.009.
Stephens, J.A., Berryhill, M.E., 2016. Older adults improve on everyday tasks after working memory training and neurostimulation. Brain Stimul 9 (4), 553–559. https://doi.org/10.1016/j.brs.2016.04.001.
Team, J., 2017. JASP. Retrieved from, Version 0.8.3.1. https://jasp-stats.org/.
Terhune, D.B., Russo, S., Near, J., Stagg, C.J., Cohen Kadosh, R., 2014. GABA predicts time perception. J. Neurosci. 34 (12), 4364–4370. https://doi.org/10.1523/jneurosci.3972-13.2014.
Turner, B.M., Sederberg, P.B., Brown, S.D., Steyvers, M., 2013. A method for efficiently sampling from distributions with correlated dimensions. Psychol. Methods 18, 368–384.
van de Ruit, M., Grey, M.J., 2019. False positives associated with responder/non-responder analyses based on motor evoked potentials. Brain Stimul. 12 (2), 314–318. https://doi.org/10.1016/J.BRS.2018.11.015.
Verghese, A., Garner, K.G., Mattingley, J.B., Dux, P.E., 2016. Prefrontal cortex structure predicts training-induced improvements in multitasking performance. J. Neurosci. 36 (9), 2638–2645.
Wiethoff, S., Hamada, M., Rothwell, J.C., 2014. Variability in response to transcranial direct current stimulation of the motor cortex. BR 7, 468–475. https://doi.org/10.1016/j.brs.2014.02.003.
Yoon, J.H., Grandelis, A., Maddock, R.J., 2016. Dorsolateral prefrontal cortex GABA concentration in humans predicts working memory load processing capacity. J. Neurosci. 36 (46), 11788–11794.